Appendix Figures and Tables

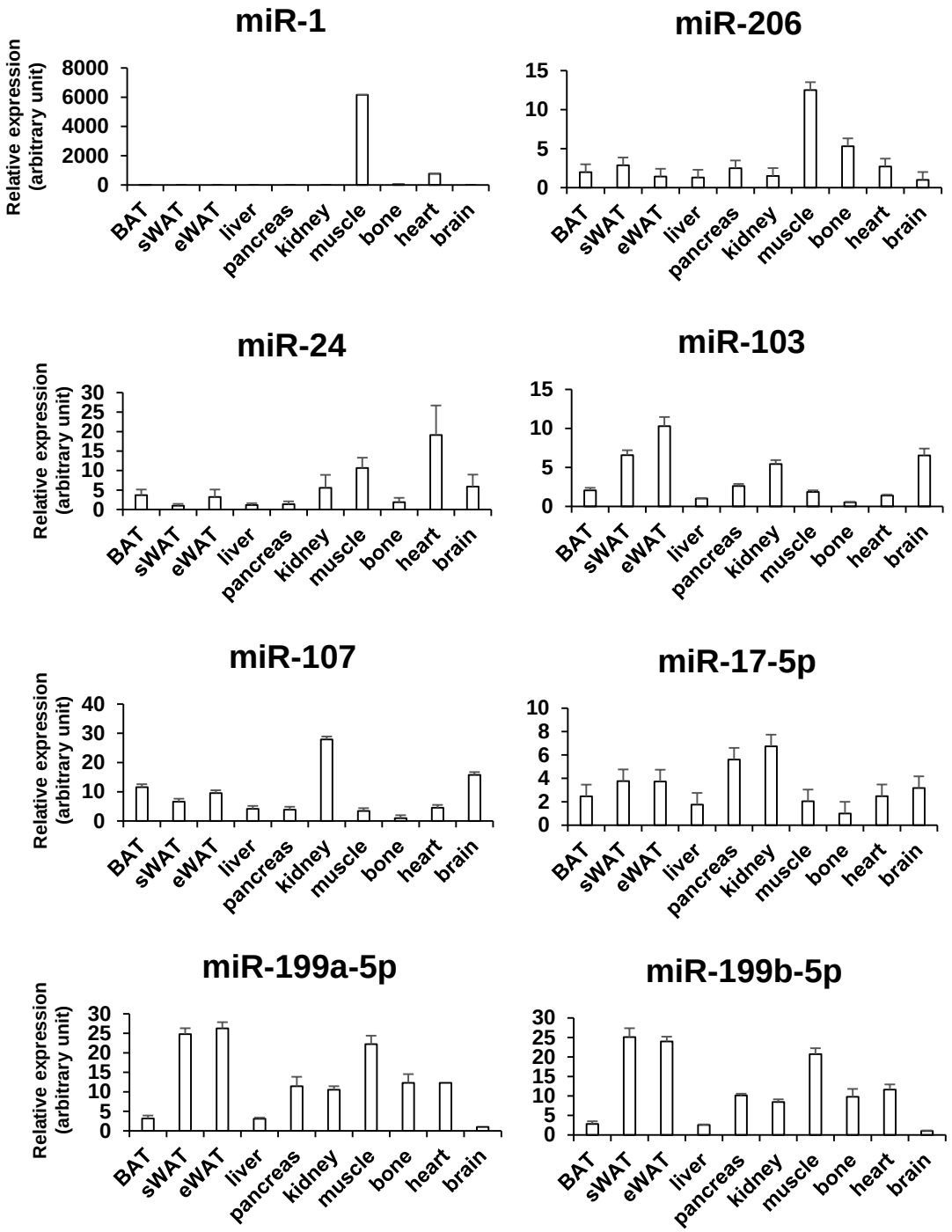

Appendix Figure S1. Tissue expression pattern of examined microRNAs candidates from microRNA array and mirBridge. Total RNAs were isolated from tissues of five-week C57BL/6 mice, and microRNAs expression were quantified by Q-RT-PCR (n=3~6). Data were analyzed with Student's t-test, and presented as mean ± SEM (*p<0.05, **p<0.01, ***p<0.001).

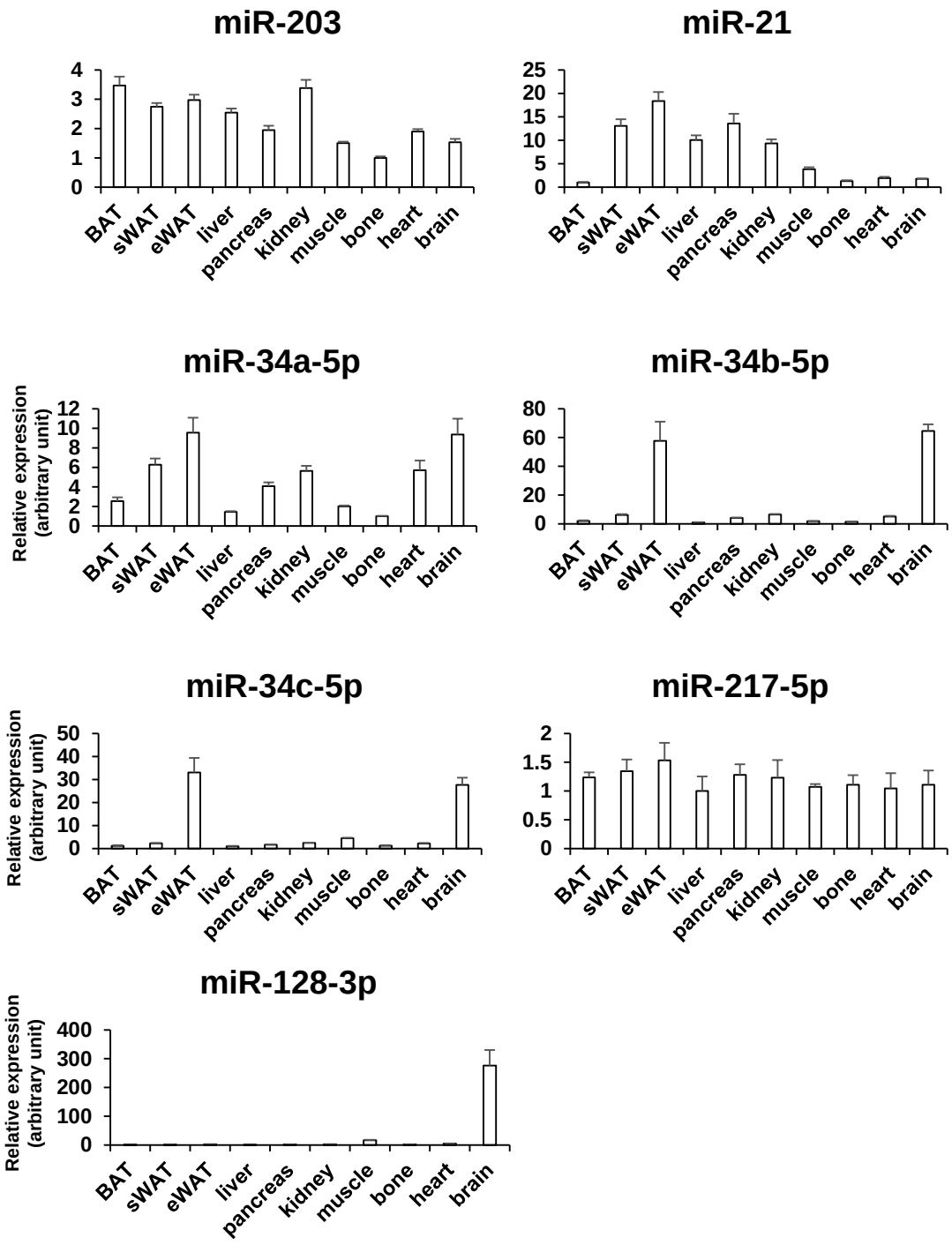

Appendix Figure S1. (continued).

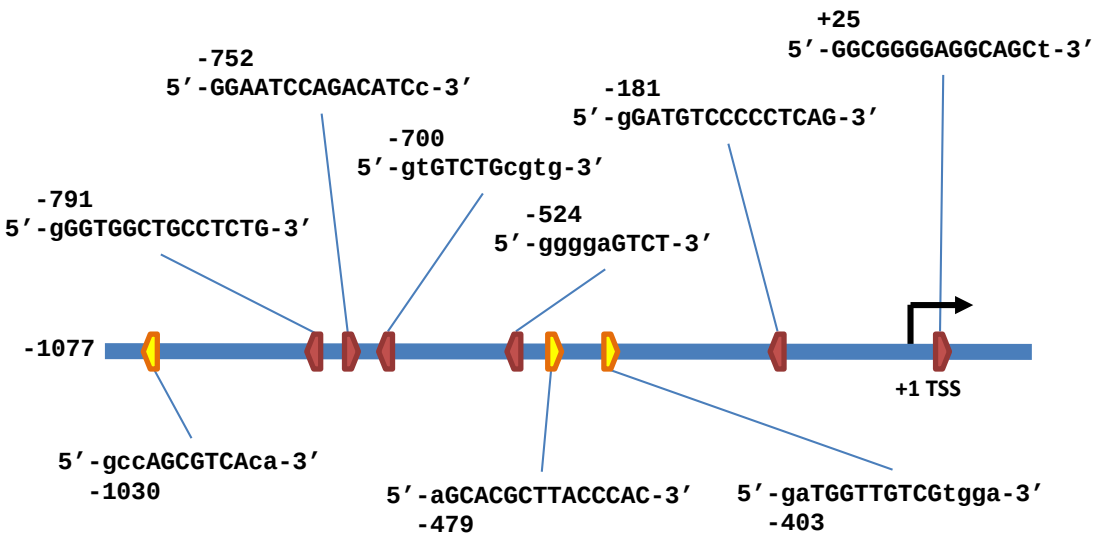

SBEs (Smad Binding Elements) for Smads-mediated transcription

CREs (cAMP Responsive Elements) for p38MAPK and cAMP-mediated transcription

SBEs and CREs include sequences in both sense and antisense directions, but only the sequences of sense strand are shown.
TSS: Transcription Start Site

Appendix Figure S2. Bioinformatics analysis of mouse miR-455 promoter. Mouse miR-455 promoter (~1 kb) was analyzed by program rVista 2.0 (http://rvista.dcode.org/) to identifiy SBEs (Smad Binding Elements) and CREs (cAMP Responsive Elements).

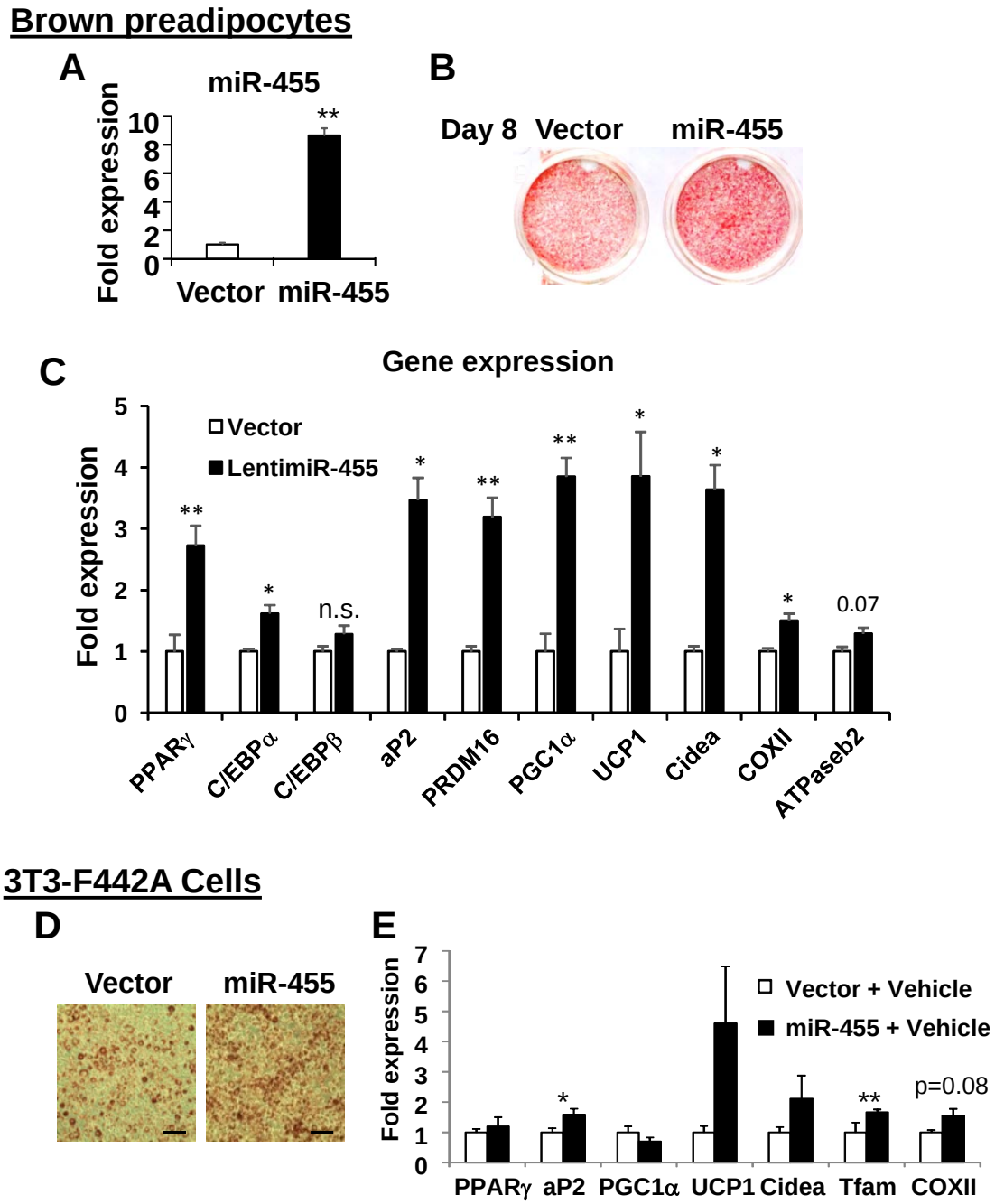

Appendix Figure S3. Overexpression of miR-455 promotes brown adipocyte differentiation *in vitro*. Brown preadipocytes and 3T3-F442A cells were transduced by lentimiR-455 or empty lentiviral vector, selected and pooled. Data were analyzed with Student's t-test, and presented as mean ± SEM of a representative from 3 independent experiments with each performed in triplicates or quadruplicates (*p<0.05, **p<0.01, ***p<0.001, n.s., non-significant).

Brown preadipocytes were differentiated by standard differentiation protocol (see Materials and Methods). (A) miR-455 overexpression on day 0, as analyzed by Q-RT-PCR. **(B)** On Day 8, cells were stained with Oil Red O; **(C)** gene expression on day 8 were analyzed by Q-RT-PCR.

F442A cells were differentiated by differentiation cocktail containing 850nM insulin and 1nM T3. (D) F442A cells were stained with Oil Red O on Day 8; scale bar, 50 μm. **(E)** RNA was harvested on Day 8 and analyzed for adipocyte gene expression by Q-RT-PCR.

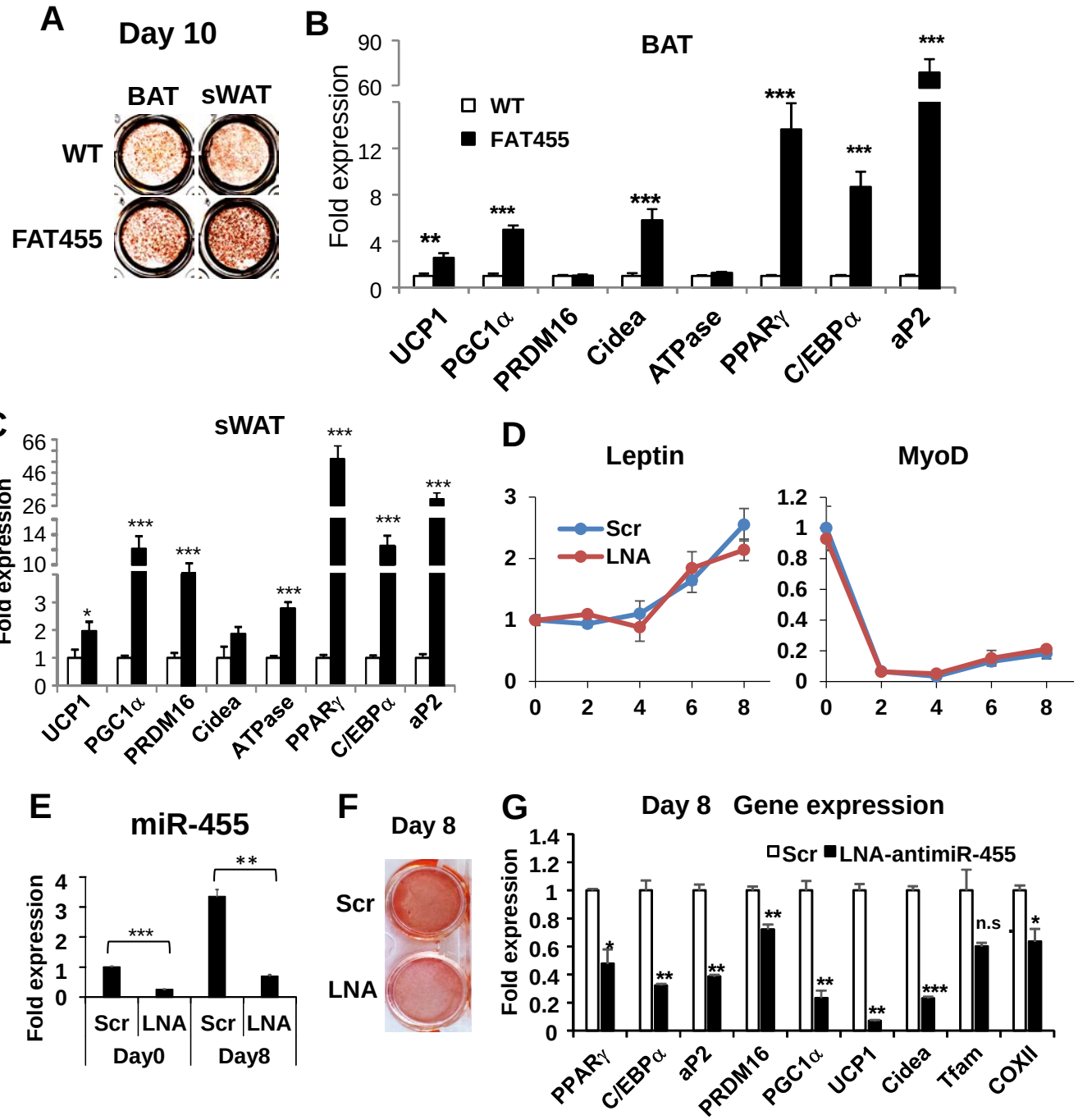

Appendix Figure S4. A-C. miR-455 enhanced brown adipocyte differentiation of sWAT-SVFs isolated from FAT455 mice. SVF were isolated from BAT and sWAT of WT and FAT455 (aP2-miR-455) mice, plated in culture dish, and induced to differentiate by standard differentiation protocol (see Materials and Methods). **(A)** On Day 10, cells were stained with Oil Red O. **(B)** Gene expression in BAT analyzed by Q-RT-PCR. **(C)** Gene expression in sWAT analyzed by Q-RT-PCR. **D-G. Knockdown of miR-455 brown preadipocytes by LNA-antimiR455 impaired their brown adipocyte differentiation.** Brown preadipocytes were transfected by LNA-antimiR-455 or scramble at 85% confluency. Two days after LNA transfection, the cells were induced to differentiate by standard protocol (**D**, as in Fig 3) or by supplementing DMEM+10% FBS with 3.3 nM BMP7 throughout differentiation process (**E-F**). **(D)** Expression of Leptin and MyoD. **(E)** LNA-antimiR-455 mediated knockdown of miR-455. **(F)** Oil Red O staining of the cells on Day 8. **(G)** Gene expression analysis by Q-RT-PCR on day 8. Data were analyzed with Student's t-test, and presented as mean ± SEM of a representative from 3 independent experiments with each performed in triplicates (*p<0.05, **p<0.01, ***p<0.001, n.s., non-significant).

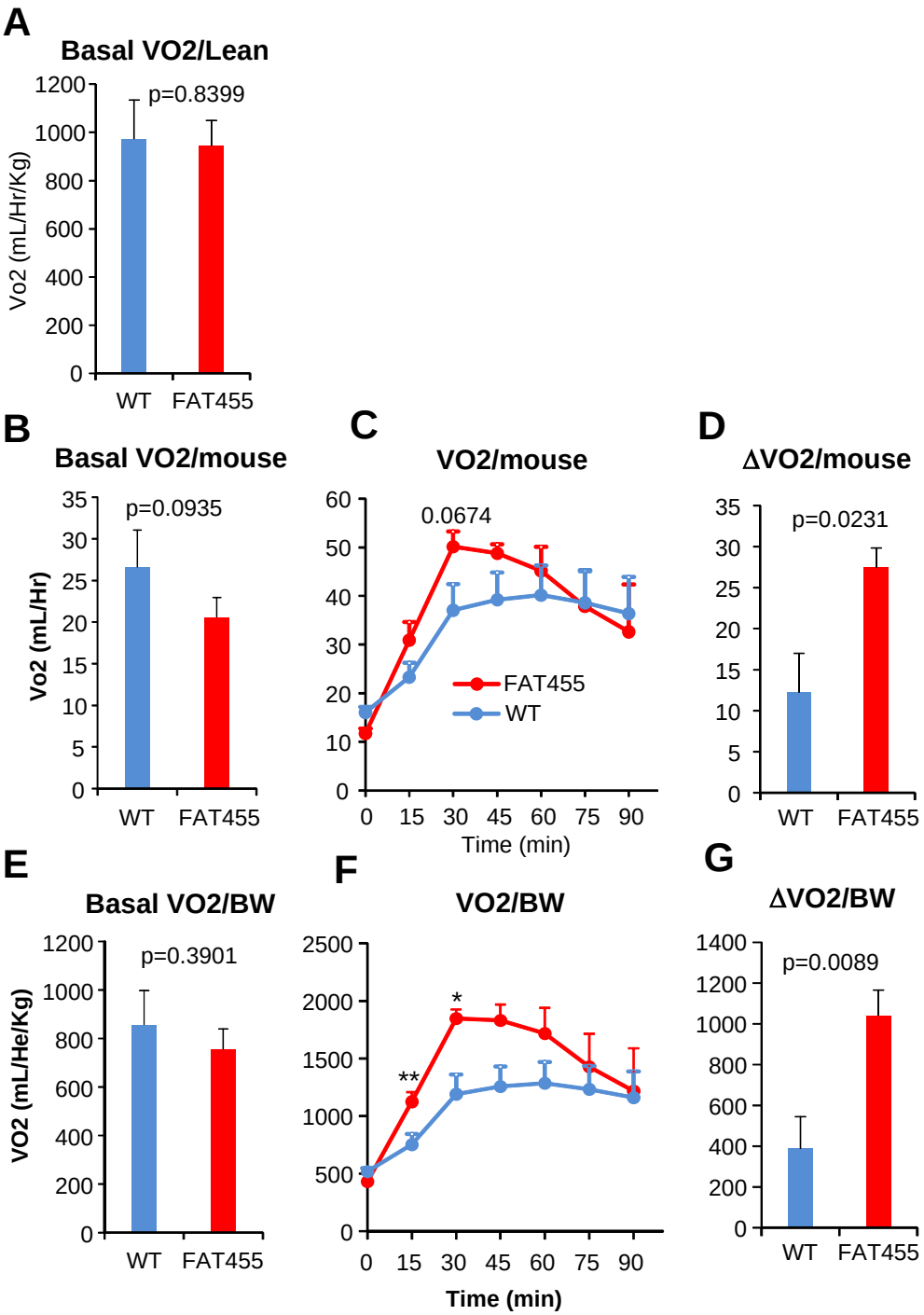

Appendix Figure S5. FAT455 mice had significantly higher maximal thermogenic capacity than WT littermates. FAT455 mice and the age-matched WT littermates were maintained at 5 ºC for 8 days to activate brown adipose tissue prior to CLAMS recording (n=6/group). Basal values (the left panels) were recorded for 30 min, followed by norepinephrine (NE) injections to maximally activate mitochondrial uncoupling. The averages of 3 basal measurements were calculated as the basal values for further calculations. After NE-injection (t0), the mice were further recorded for 90 min with 15 min interval between each recording.

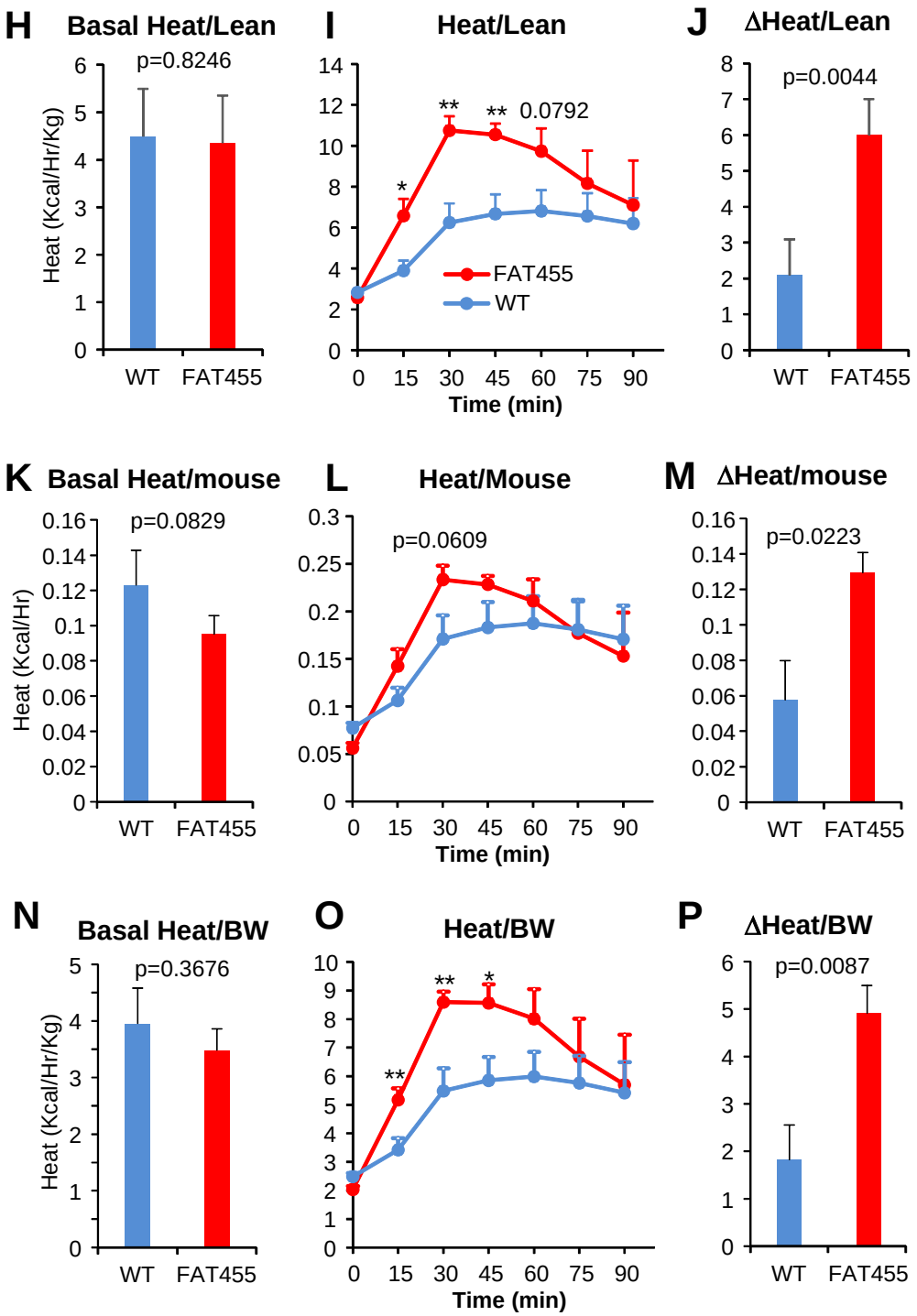

Appendix Figure S5. **(continued)** For all the values (VO_2 **(A-G)** and heat **(H-P),** three types of data were presented: per lean mass, per mouse and per body weight (BW). Time course of NE-induced oxygen consumption (VO_2) and heat production (Heat) were also present (middle panels). The maximal values (VO_2 and heat) were calculated as the average of the 3 highest values after NE-injection (t30, t45 and t60). The maximal thermogenic capacity (right panels) were calculated by comparing the absolute difference between basal values and the maximum NE-induced values (ΔVO2, and ΔHeat). The body composition of the mice were determined by Dual Energy X-ray Absorptiometry (DEXA). Data were analyzed with Student's t-test, and presented as mean ± SEM (n = 6/group. *p<0.05, **p<0.01, ***p<0.001).

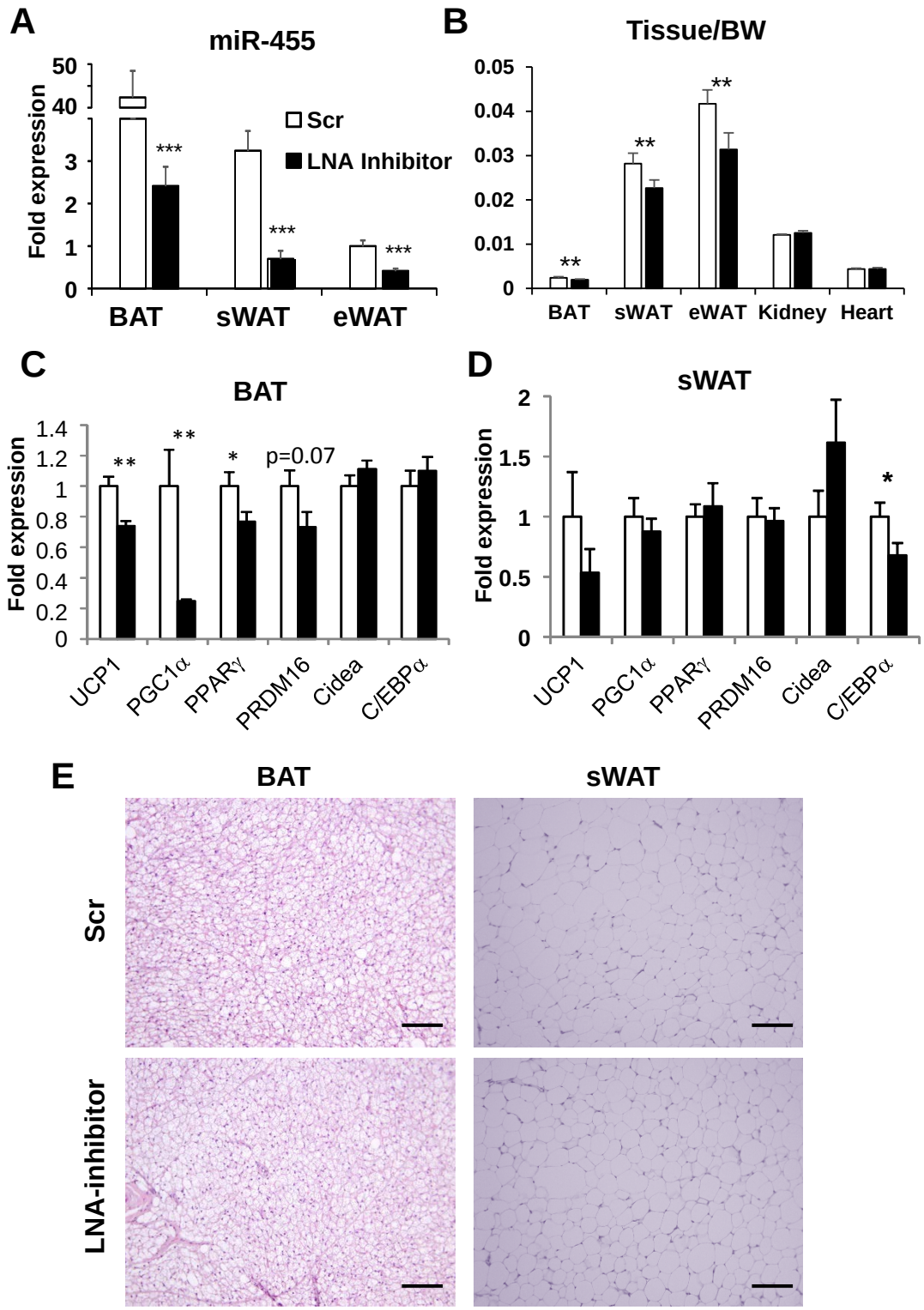

Appendix Figure S6. Depletion of miR-455 inhibited brown fat development and function. C57BL/6 mice at age of 5 weeks with equal body weight were injected intraperitoneally with LNA-antimiR455 inhibitor or scramble (scr) at dosage of 10mg/Kg body weight, once a week, for 11 weeks. The mice were sacrificed afterwards, tissues were dissected, and gene expression in adipose tissue was analyzed by Q-RT-PCR. Data were analyzed with Student's t-test, and presented as mean ± SEM (n=6/group. *p<0.05, **p<0.01, ***p<0.001). **(A)** miR-455 expression. **(B)** Tissue weights relative to whole body weight. **(C)** Brown and general adipogenic gene expression in BAT. **(D)** Brown and general adipogenic gene expression in sWAT. **(E)** Histology by H&E staining of tissue sections. Scale bar, 50 μm.

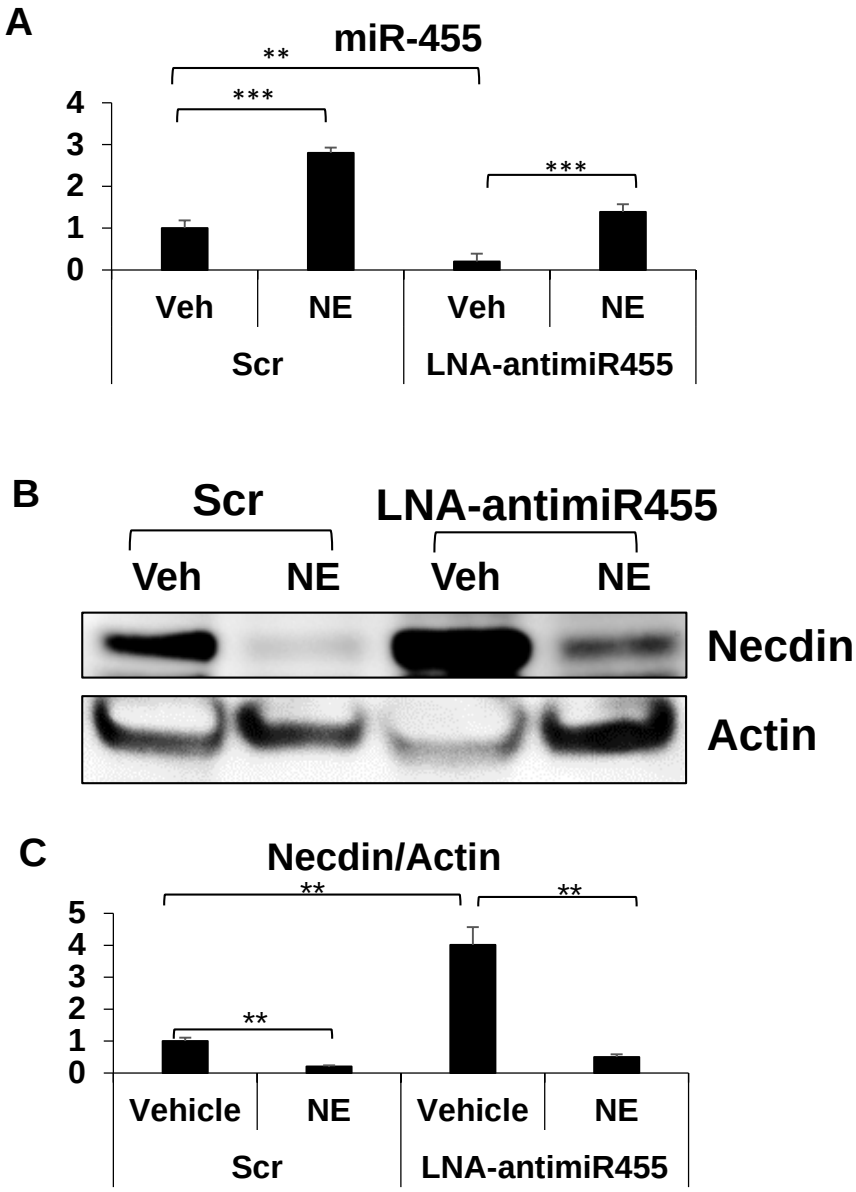

Appendix Figure S7. miR-455 mediates NE's effect on Necdin protein expression. Brown preadipocytes were transfected with LNA-antimiR455 or Scramble control at 85% confluence. 24 hours after transfection, the cells were treated with norepinephrine (NE) for 48 hours. Then RNA and protein were isolated for Q-RT-PCR and western blot analysis. Expression of miR-455 (A) and one representative blot (B) was shown. Densitometry (C) was performed from three blots.

Discussion: NE treatment significantly suppressed Necdin protein level compared to vehicle treatment, and LNA-antimiR455 transfection markedly upregulated the protein level of Necdin compared to Scamble transfection. Since miR-455 expression was also induced by NE treatment, in cells transfected with LNA-antimir455 and treated with NE, miR-455 expression was compromised. Consequently, cells receiving LNA-antimiR455 and NE treatment displayed an intermediate level of Necdin protein expression between NE treatment alone and LNA-antimiR455 transfection alone. These data suggest that miR-455 mediates at least part of NE's effect on Necdin protein expression.

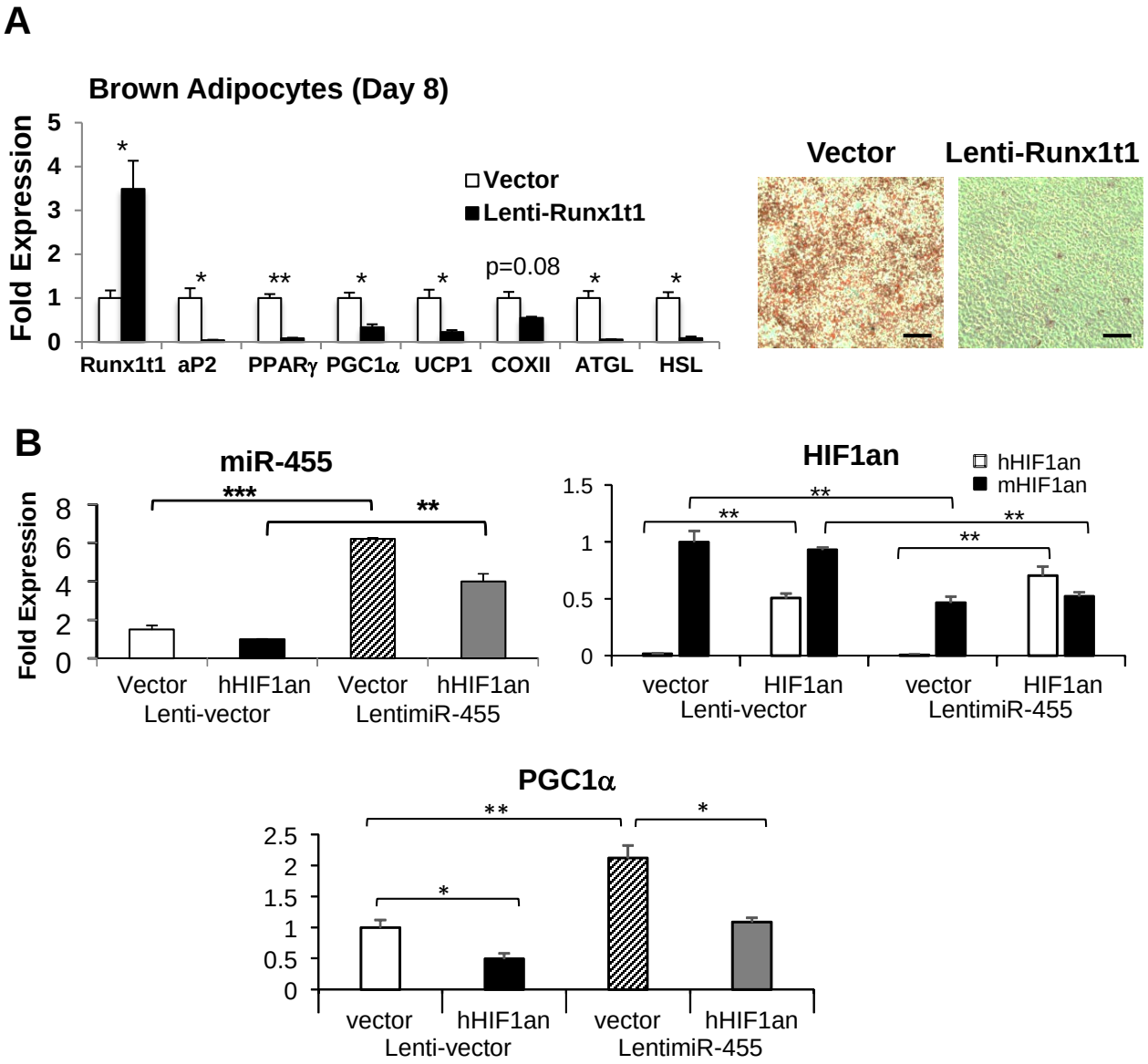

Appendix Figure S8. A. Overexpression of Runx1t1 inhibited brown adipocyte differentiation. Runx1t1 was overexpressed in brown preadipocytes via lentiviral delivery, empty vector was used as control. Stably transduced cells were selected and pooled. On Day 8, gene expressions were analyzed by Q-RT-PCR, and cells were stained by Oil Red O. Scale bar, 50 μm. Data were analyzed with Student's t-test, and presented as mean ± SEM of a representative from 3 independent experiments with each performed in triplicates (*p<0.05, **p<0.01, ***p<0.00).

B. Overexpression of HIF1an blocked miR-455 from inducing PGC1α. A human HIF1an transgene lacking its native 3'UTR was overexpressed at the level comparable to the endogenous mouse HIF1an, on top of miR-455 overexpression in brown preadipocytes. Empty vectors were used as controls. On Day 0, miR-455 and gene expressions were analyzed by Q-RT-PCR. For analysis of endogenous mouse (mHIF1an) and ectopically expression human HIF1an (hHIF1an) transgenes, specific primers targeting their cDNA regions were used, which could distinguish the transgenes from the endogenous genes that would be suppressed by miR-455 via its native 3'UTR.

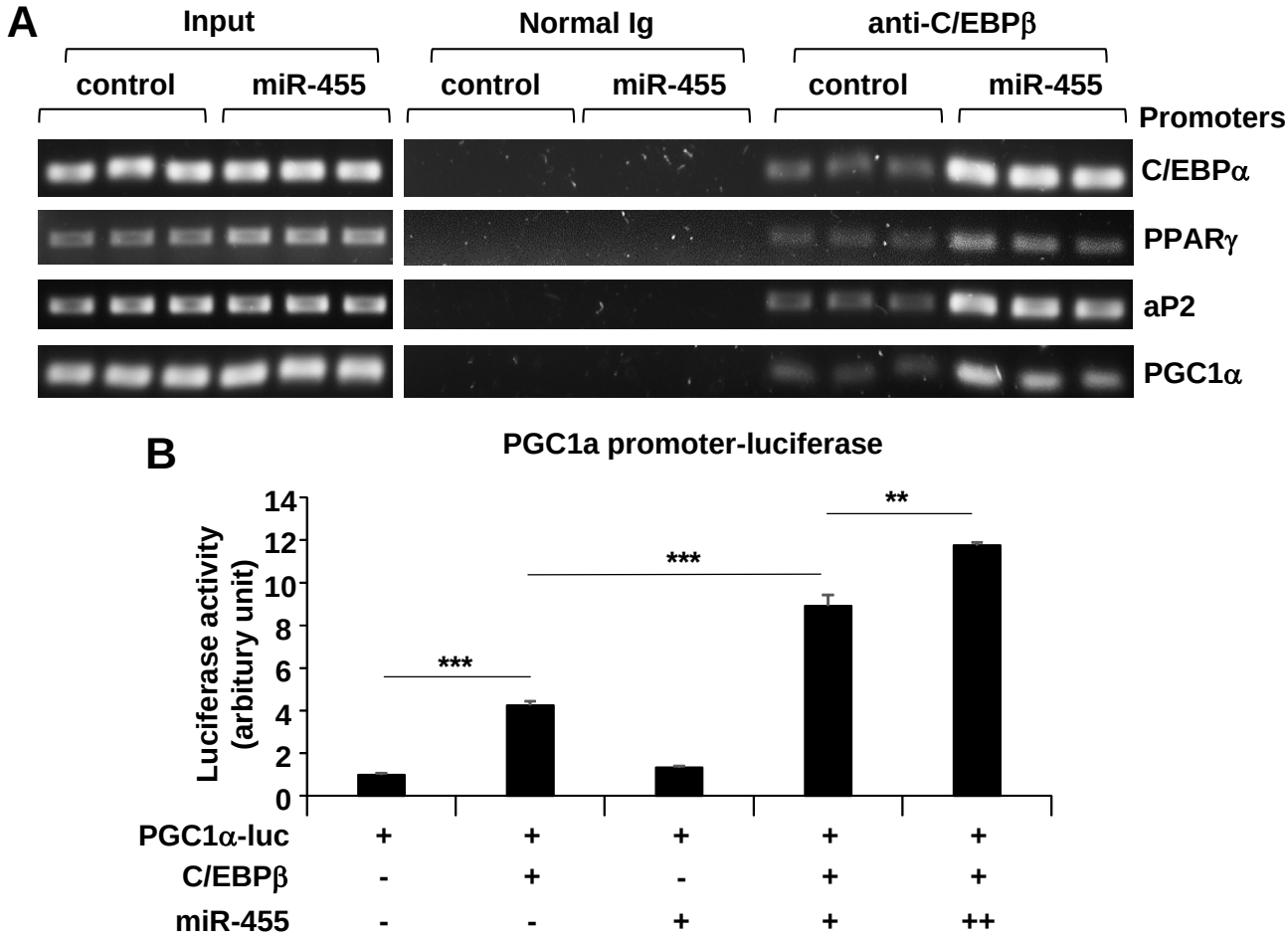

Appendix Figure S9. miR-455 potentiates C/EBPβ transcriptional activity.

(A) Brown preadipocytes overexpressing miR-455 or control (vector) were differentiated by standard differentiation protocol. 5 hours after differentiation, cells were crosslinked by formaldehyde and harvested for total protein and genomic DNA for ChIP assay. ChIP assay was performed according to standard ChIP protocol using anti-C/EBPβ antibody and primer pairs flanking the CCAAT binding motif on the promoters of C/EBPα, PPARγ, aP2, and flanking the cAMP binding element (CRE) on PGC1α promoter. 20% total lysates were used as input loading control.

Discussion: Anti-C/EBPβ antibody significantly enriched the promoter DNAs of C/EBPα, PPARγ , aP2 and PGC1α, showing that C/EBPβ efficiently bound to the promoter regions of these genes. Importantly, miR-455-overexpressing cells had significantly increased enrichment of these promoter DNA, demonstrating that miR-455 overexpression significantly enhanced the binding of C/EBPβ to the CAAT element and CRE of these gene promoters, presumably through miR-455-mediated suppression of Runx1t1.

(B) PGC1α promoter(2kb)-luciferase (firefly) construct was cotransfected with C/EBPβ, miR-455 or control expression vectors and TK-Rluciferase (renilla) into brown preadipocytes (TK-Rluc is presented in all transfection as internal control) 24 hours after transfection, the cells were treated with 10uM forskolin in serum-free condition for 12 hours. The cell lysates were then harvested for luciferase activity assay. The firefly luciferase activity was normalized to renilla luciferase acticity. Student's t-test was used for statistical analysis, and mean ± SEM from quadruplicates are shown.

Discussion: Cotransfection of C/EBPβ significantly activated PGC1α promoter, consistent with previous report [29]. Importantly, cotransfection of miR-455 further increased PGC1α promoter activity in a dose-dependent manner. However, in the absence of C/EBPβ, miR-455 had only minimal effect on PGC1α promoter activity. This data demonstrated that miR-455 potentiated C/EBPβ on the transactivation of PGC1α promoter.

A

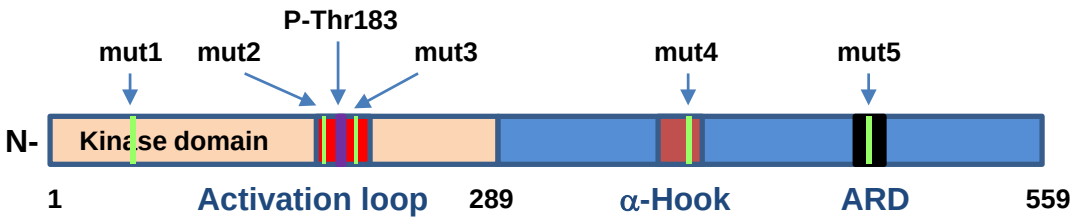

B

```
MRRLSSWRKM ATAEKQKHDG RVKIGHYILG DTLGVGTFGK VKVGKHELTG HKVAVKILNR  60
                                                          Mut1(Asn59)

QKIRSLDVVG KIRREIQNLK LFRHPHIIKL YQVISTPSDI FMVMEYVSGG ELFDYICKNG 120
RLDEKESRRL FQQILSGVDY CHRHMVVHRD LKPENVLLDA HMNAKIADFG LSNMMSDGEF 180
                                                      Mut2(Asn173)
   Activation loop
LRTSCGSPNY AAPEVISGRL YAGPEVDIWS SGVILYALLC GTLPFDDDHV PTLFKKICDG 240
Phos-Thr183 Mut3(Asn189)

IFYTPQYLNP SVISLLKHML QVDPMKRAAI KDIREHEWFK QDLPKYLFPE DPSYSSTMID 300
DEALKEVCEK FECSEEEVLS CLYNRNHQDP LAVAYHLIID NRRIMNEAKD FYLATSPPDS 360
FLDDHHLTRP HPERVPFLVA ETPRARHTLD ELNPQKSKHQ GVRKAKWHLG IRSQSRPNDI 420
                          a-Hook   Mut4(Asn393)

MAEVCRAIKQ LDYEWKVVNP YYLRVRRKNP VTSTFSKMSL QLYQVDSRTY LLDFRSIDDE 480
            ARD    Mut5(Asn439)

ITEAKSGTAT PQRSGSISNY RSCQRSDSDA EAQGKPSDVS LTSSVTSLDS SPVDVAPRPG 540
SHTIEFFEMC ANLIKILAQ                                              559
```

Appendix Figure S10. A. Functional domains of AMPKα1.
B. Amino acid sequence of human AMPKα1. Phosphorylation of Thr183 in AMPKα1 (conventionally named as Thr172 after initial identification in AMPKα2) and the five Asn-to-Ala mutations were highlighted in red. Asn173 (mutant2) and Asn189 (mutant3) are located within the activation loop, the kinase center of AMPKα1. Asn393 (Mutant4) is located in the α-hook domain, which is responsible for interacting with the γ-subunit and mediating the protection of Thr183 against dephosphorylation by phosphatases. Asn439 (mutant5) is located in a putative ankyrin-repeat domain (ARD), a potential hydroxylation target. Asn59 (mutant1) could be spatially located near the Thr183 kinase center in 3D structure. Therefore, hydroxylation of these chose Asn residues could potentially trigger AMPKα1 conformational change and thereby modulate its activity.

microRNA	Known function or signaling
miR-1/206	Skeletal muscle development
miR-24	Tumorigenesis
miR-103/107	Insulin sensitivity, glucose homeostasis, lipid metabolism
miR-17-5p	BMP signaling-mediated myocardial differentiation; accelerate adipocyte differentiation
miR-199	BMP-mediated microRNA processing
miR-455-5p	Expressed in brown adipocytes
miR-365	Brown adipogenesis
miR-21	TGFβ/BMP mediated microRNA processing, myogenesis
miR-203.1	Tumor suppressor
miR-34	Tumorigenesis
miR-128	Associated with impaired amyloid degradation in Alzheimer's Disease
miR-217	Tumor suppressor; promotes fat accumulation in hepatocytes

Appendix Table S1. microRNAs identified by combining microRNA array and mirBridge analysis, using BMP7/Vehicle or Vehicle/BMP7 fold >1.5 and p<0.05 as cutoff, respectively.

Gender	Age	BMI
M	32	29.8
M	42	33
M	48	30.4
F	49	25.4
F	44	32.3
F	44	23.5
F	71	33.5

Appendix Table S2. Information on human subjects from whom sWAT and BAT were isolated to determine miR-455 and UCP1 expression (see Fig 1F,G).

miR-455 Target Genes	Seed region position in 3’UTR	Sequence pairing of target region (top) and microRNA (bottom)
HIF1an	HIF1an 3’UTR Position 106-112 mmu-miR-455	5' ...GCACGCUGCACUUAAUGGACUGG...3’ | 3' CACAUAUACGGGCACCUGACG 5’
	HIF1an 3' UTR Position 1610-1617 mmu-miR-455	5' ...GCUUACAGCGCCCCAUGGACUGA...3’ |	||| ||||||| 3' CACAUAUACGGGCACCUGACG 5’
Necdin	Necdin 3’UTR Position 430-436 mmu-miR-455	5' ...AUCCAUGUG-GAAUGGACUGA...3' | || ||	||||||| 3' CACAUAUACGGGCACCUGACG 5'
	Necdin 3’UTR Position 445-451 mmu-miR-455	5' ...ACUGAUUUGAAC-UGGACUGU...3' |||||	||||||| 3' CACAUAUACGGGCACCUGACG 5'
Runx1t1	Runx1t1 3' UTR Position 3666-3672 mmu-miR-455	5' ...UUUUUUUUCCUUAGUUGGACUGU...3’ |	| 3' CACAUAUACGGGCACCUGACG 5’

Appendix Table S3. miR-455 target sequences in the 3’UTR of target genes.

Cloning		
miR-455 cloning primer	Forward	ATTGGCATCATCTCTAGCCTCC
	Reverse	TCCTGGGCCTCACCCTACTT
Genotyping		
aP2-miR-455 mice Genotyping	Forward	CATGCCTTCTTCTCTTTCCTACAG
	Reverse	TCCTGGGCCTCACCCTACTT
microRNA Q-RT-PCR		
miR-455-5p	Forward	TATGTGCCTTTGGACTACATCG
miR-455-3p (miR-455)	Forward	GCAGTCCACGGGCATATACAC
Mouse *RNU6*	Forward	TGGCCCCTGCGCAAGGATG
Human *miR-455*	Forward	GCAGTCCATGGGCATATACAC
Human *RNU1*	Forward	CGACTGCATAATTTGTGGTAGTGG
miR universal reverse primer	Reverse	TCAGTGCAGGGTCCGAGGT
gene Q-RT-PCR		
Arbp (38B4)	Forward	TTTGGGCATCACCACGAAAA
	Reverse	GGACACCCTCCAGAAAGCGA
Pparγ	Forward	TCAGCTCTGTGGACCTCTCC
	Reverse	ACCCTTGCATCCTTCACAAG
Cebpα	Forward	CAAGAACAGCAACGAGTACCG
	Reverse	GTCACTGGTCAACTCCAGCAC
aP2	Forward	GATGCCTTTGTGGGAACCT
	Reverse	CTGTCGTCTGCGGTGATTT
Pgc1α	Forward	CCCTGCCATTGTTAAGACC
	Reverse	TGCTGCTGTTCCTGTTTTC
UCP1	Forward	AGGCTTCCAGTACCATTAGGT
	Reverse	CTGAGTGAGGCAAAGCTGATTT
Prdm16	Forward	CAGCACGGTGAAGCCATTC
	Reverse	GCGTGCATCCGCTTGTG
Cidea	Forward	ATCACAACTGGCCTGGTTACG
	Reverse	TACTACCCGGTGTCCATTTCT

Appendix Table S4. The sequences of primers used for cloning, genotyping, and Q-RT-PCR.

gene Q-RT-PCR		
Tfam	Forward	GTCCATAGGCACCGTATTGC
	Reverse	CCCATGCTGGAAAAACACTT
COX5b	Forward	GCTGCATCTGTGAAGAGGACAAC
	Reverse	CAGCTTGTAATGGGTTCCACAGT
NRF1	Forward	CAACAGGGAAGAAACGGAAA
	Reverse	GCACCACATTCTCCAAAGGT
COXII	Forward	CCATCCCAGGCCGACTAA
	Reverse	AATTTCAGAGCATTGGCCATAGA
CytoC1	Forward	GCTACCCATGGTCTCATCGT
	Reverse	CATCATCATTAGGGCCATCC
CD36	Forward	TGTGTTTGGAGGCATTCTCA
	Reverse	TTTTGCACGTCAAAGATCCA
ATGL	Forward	TGTGGCCTCATTCCTCCTAC
	Reverse	TCGTGGATGTTGGTGGAGCT
HSL	Forward	CACCCATAGTCAAGAACCCCTTC
	Reverse	TCTACCACTTTCAGCGTCACCG
Necdin	Forward	ATATGACTTCAACTGGCACAGGAAG
	Reverse	GGGTGCTAAGTGCCTACACTGAG
Runx1t1	Forward	CCGAACTGTGGTTTCTTGTTTATCC
	Reverse	ATTCACAGGTTGACAGACCATACATT
Runx1t1 transgene	Forward	ATGCCTGATCGTACCGAGAAG
	Reverse	GTCGTTGGCGTAAATGAGCTG
HIF1an	Forward	GCACTAGTATTGCACGCTGCAC
	Reverse	CAGGGCCATGGCAAGAGTC
Human *HIF1an* transgene	Forward	CCCAATGTACTGGTGGCATCAC
	Reverse	GTTGTATCGGCCCTTGATCATT
Mouse&Human common primer *HIF1an*	Forward	GGCTCCCACCCCTAAGAGAAT
	Reverse	GCCCCACCTCTTGTGGGTT
Human *UCP1*	Forward	ACCGCAGGGAAAGAAACAGC
	Reverse	TCAGATTGGGAGTAGTCCCT
Human *18S*	Forward	TCAACTTTCGATGGTAGTCGCCGT
	Reverse	TCCTTGGATGTGGTAGCCGTTTCT
ChIP primers for promoter analysis (C/EBPβ binding)		
C/EBPα promoter	Forward	TCCCTAGTGTTGGCTGGAAG
	Reverse	CAGTAGGATGGTGCCTGCTG
PPARγ promoter	Forward	TTCAGATGTGTGATTAGGAG
	Reverse	AGACTTGGTACATTACAAGG
aP2 promoter	Forward	CCTCCACAATGAGGCAAATC
	Reverse	CTGAAGTCCAGATAGCTC
PGC1α promoter	Forward	GGGCTGCCTTGGAGTGACGTC
	Reverse	AGTCCCCAGTCACATGACAAAG

Appendix Table S4 (continued)